(Received 1 May 2025, Accepted 16 June 2025, Scheduled 7 July 2025)

Switchable Tunable Absorber Based on Graphene and Vanadium Dioxide

Baojun Chen[1], Tianyu Jiao[2], Mengqiu Qian[2], Yanjie Ju[1,*], and Yanbing Xue[1]

[1]*School of Electrical Engineering, Dalian Jiaotong University, Dalian 116028, Liaoning, China*
[2]*School of Railway Intelligent Engineering Engineering, Dalian Jiaotong University, Dalian 116028, Liaoning, China*

ABSTRACT: This article addresses the challenges associated with poor tunability and the single absorption function in absorbers. To address these challenges, we designed a dual-band switchable tunable absorber utilizing graphene and vanadium dioxide. The proposed absorber exploits the phase transition characteristics of vanadium dioxide to achieve absorption in the low-frequency band when it is in the dielectric state and absorption switching in the high-frequency band after phase transition. Furthermore, the Fermi level is altered by applying a bias voltage to the graphene, resulting in reduced square resistance. This mechanism allows tuning of the absorption frequency when the vanadium dioxide is in the dielectric state and adjustment of the absorption bandwidth when it is in the metallic state. Simulation results reveal that when the vanadium dioxide is in the dielectric state, the absorption rate exceeds 90% within the 20.0–27.7 GHz range. At this time, increasing the Fermi level of the graphene alters the absorption frequencies to 11 GHz and 42 GHz, respectively. Conversely, when the vanadium dioxide is in the metallic state, the absorption rate exceeds 90% within the 31.1–48.7 GHz range. Thus, elevating the Fermi level of the graphene leads to absorption band tuning at higher frequencies. This absorber demonstrates strong tunability and multifunctional absorption capabilities, offering outstanding practical application value.

1. INTRODUCTION

Traditional absorbers suffer from the limitation of fixed absorption frequencies, requiring structural reconfiguration for operation across various frequency ranges [1]. This not only increases system complexity and cost, but also prevents them from meeting dynamic electromagnetic control requirements — particularly those demanding intelligent adaptation in complex electromagnetic environments. To address this issue, adjustable absorbers have been explored, applying thermal sensitivity [2], photosensitivity, active devices [3], and graphene materials [4]. While electrically tunable lumped components offer advantages in switching speed and fabrication simplicity, they exhibit fundamental limitations in achieving multifunctional switching across broad operational ranges. In contrast, graphene and vanadium dioxide (VO_2) demonstrate marked and continuous variations in conductivity/permittivity under external stimuli, proving that they are more effective for realizing tunable broadband absorption and multifunctional switching capabilities. Graphene is a two-dimensional material with excellent electrical properties. By applying a bias voltage, the impedance can be changed, allowing graphene to be used as a material for adjustable absorbers. Vanadium dioxide stands out as an excellent phase-change material [5]. By altering the ambient temperature to 68°, it undergoes a phase change and tunes the absorption rate of the absorbers. Currently, existing research on vanadium dioxide tunable absorbers mainly focuses on the terahertz band [6–8]. Their tunability is manifested in two aspects. First, at room temperature, vanadium dioxide medium state achieves a total reflection function. However, at a high temperature, after transforming into a metal state, it achieves a multi-frequency or broadband absorption function [9–11]. The second aspect is to achieve tuning of the absorption rate of the absorber by regulating the conductivity of the vanadium dioxide [12–16]. Some scholars have used adjustable absorbers constructed with vanadium dioxide to realize multi-frequency absorption effects when the vanadium dioxide is in the dielectric state. These absorbers achieve broadband absorption when the vanadium dioxide transitions to the metallic state [17, 18], greatly improving the tunable absorption ability. Recently, some researchers have simultaneously used vanadium dioxide and graphene materials to design tunable absorbers [13, 19, 20]. Although the absorption frequency can be tuned before and after the vanadium dioxide phase transition, there are considerable limitations. The graphene must be loaded with voltage to work properly, resulting in reduced practical application capabilities. While existing tunable absorbers predominantly function in the terahertz regime, we propose a dual-band switchable absorber based on vanadium dioxide (VO_2) and graphene, operating primarily within the K-band (18–27 GHz) and Ka-band (27–40 GHz). In the medium state of vanadium dioxide at room temperature, the absorber achieves low-frequency broadband absorption. Following the high-temperature phase transition of the vanadium dioxide, the absorber switches to high-frequency broadband absorption. Moreover, increasing the Fermi level of graphene enables a frequency shift in the absorber's response. Additionally, elevating graphene's Fermi level induces a controllable frequency shift in the absorption response. This approach ac-

* Corresponding author: Yanjie Ju (746610878@qq.com).

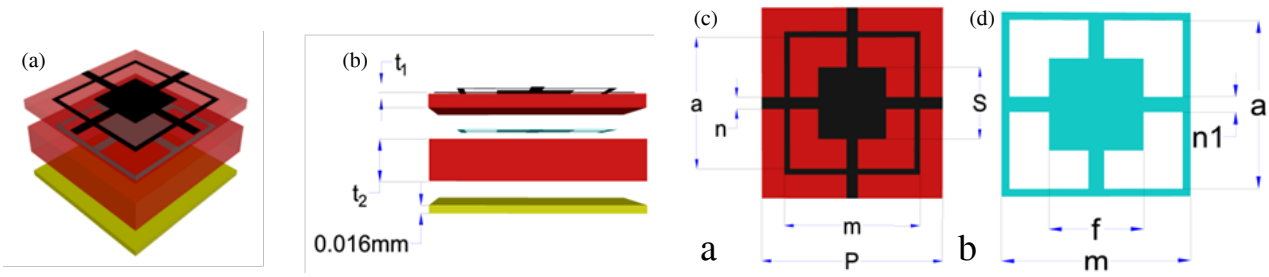

FIGURE 1. Overall structure diagram and views of each part of the absorber unit structure. (a) Unit structure diagram. (b) Side view. (c) Pattern fossil graphene surface. (d) Patterned vanadium dioxide diagram.

tively combines thermal control of VO_2 states with electrostatic tuning of graphene's Fermi level, offering significant potential for 5G/6G interference suppression (e.g., 28/39 GHz channels) and dynamic radar camouflage applications.

2. DESIGN, SIMULATION, AND ANALYSIS

2.1. Design of the Absorber

The absorber unit structure designed in this article is presented in Fig. 1. The unit consists of five layers, arranged from top to bottom as structured graphene, PET dielectric layer, structured vanadium dioxide, PET dielectric layer, and metal ground layer.

2.2. Analysis and Simulation of Absorber

The square resistance of the vanadium dioxide used in this article is 0.5 MΩ/□ in the medium state, while the resistance after phase transition is 75 Ω/□ [3]. Ref. [4] states that in the centimeter band, the resistance of graphene is approximately equivalent to a resistive surface with a resistance of 2370 Ω/□. However, after entering the millimeter wave band, the imaginary part of the graphene impedance gradually increases, which has a substantial impact on the equivalent impedance. In Unit 1 of Fig. 1, the patterned vanadium dioxide film and graphene surface are both designed as composite structures containing square rings, crosses, and squares. This type of structure maximizes the stability of the real part of the equivalent impedance. The difference between the two patterns is that the cross-shaped arms on the graphene surface are not wrapped by square rings. This allows adjacent unit structures to be connected to the graphene, facilitating the application of bias voltage to regulate the Fermi level of the graphene. Additionally, the PET medium between the graphene and vanadium dioxide provides a substrate for graphene processing and also separates the two, thus avoiding direct contact and mutual interference as a loss material. The lower layer of PET serves as a loss medium, supporting and dissipating electromagnetic wave energy.

According to the theory of equivalent circuits, an equivalent circuit model is constructed for the designed unit. The materials of each part of the unit structure are equivalent to the series-parallel form of RLC components [21–23]. Fig. 2 displays the equivalent circuit model of the vanadium dioxide metal state in this design.

When the patterned VO_2 is in the dielectric state, it is equivalent to a special transmission line model. In the metallic

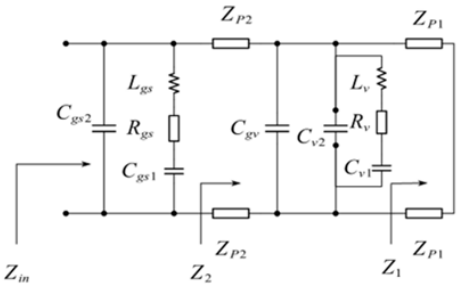

FIGURE 2. Equivalent circuit model of the vanadium dioxide metal state.

state, the square ring and cross are equivalent to inductance L_v and capacitance C_{v1} between adjacent units, and its resistance $R_v = R_V A_v/S_v$ is determined by the area ratio of the square resistance occupied, while C_{v2} represents the capacitance among the square ring, the cross, and the block inside the unit. The equivalent resistance of the patterned graphene depends on the proportion of the actual area A to the square S, with a value of $R_{gs} = R_G A_g/S_g$. The surface cross arm and square ring are equivalent to the parallel inductance L_{gs}, and the capacitance between unit structures is C_{gs1}. Additionally, C_{gs2} represents the capacitance between the square ring and cross with the square inside the unit.

The two-layer PET medium is equivalent to a transmission line with impedances of Z_{P1} and Z_{P2}, which are dependent on its characteristic impedance Z_{PET} and transmission constant k_{PET} [6]. They can be expressed as in(1)–(4):

$$Z_{P1} = jZ_{PET}\tan(k_{PET}t1). \quad (1)$$

$$Z_{P2} = jZ_{PET}\tan(k_{PET}t2). \quad (2)$$

Among them, Z_{PET} can be represented as:

$$Z_{PET} = \omega\mu_0/k_{FR4}. \quad (3)$$

k_{PET} can be expressed as:

$$k_{PET} = \omega\sqrt{\mu_0\varepsilon_{PET}\varepsilon_0}. \quad (4)$$

When the vanadium dioxide is in a metallic state, the interaction between the graphene and vanadium dioxide layers generates capacitance, which is equivalent to C_{gv}. The metal substrate is used to reduce the transmission coefficient, ignoring its impedance characteristics. The input impedance of the unit structure is equivalent to Z_{in}

$$Z_{in} = R + jX. \quad (5)$$

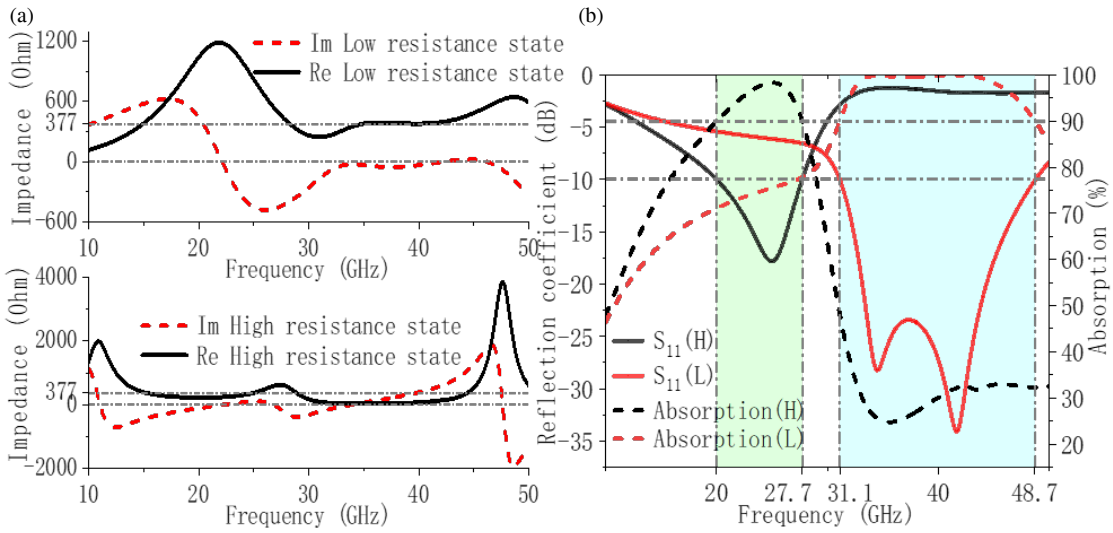

FIGURE 3. (a) Input impedance results of absorber before and after phase transition. (b) Curves of absorber absorption and reflection coefficient before and after phase transition.

When electromagnetic waves are incident from free space on the surface of the absorbing structure, the reflection coefficient can be determined as follows:

$$S_{11} = Z_{in} - Z_0 / Z_{in} + Z_0. \tag{6}$$

Here, Z_0 is the free-space characteristic impedance, which is approximately:

$$Z_0 = \sqrt{\mu_0/\varepsilon_0} = 120\pi \approx 377\,\Omega. \tag{7}$$

The absorption rate can be calculated using (8):

$$Abs = 1 - |S_{11}|^2. \tag{8}$$

Furthermore, the structure undergoes optimization using simulation software, employing periodic boundary conditions and Floquet port excitation. An open boundary is set along the Z-axis, using a frequency domain solver. The optimized unit structure features a side length of $P = 8\,\text{mm}$, a square side length of $s = 2\,\text{mm}$ for the graphene patterns, and a strip width of $n = 0.5\,\text{mm}$. The outer side length of the square ring structure is $m = 5.8\,\text{mm}$, and the inner side length is $a = 4.8\,\text{mm}$. The upper PET layer possesses a relative dielectric of $2.8(1 - j0.02)$, with a thickness of $t1 = 0.05\,\text{mm}$. The patterned VO_2 square side length $f = 1.7\,\text{mm}$ and strip width $n1 = 0.5\,\text{mm}$. The lower PET layer has a thickness of $t2 = 1.2\,\text{mm}$, and the metal substrate is composed of copper with a thickness of 0.016 mm. The proposed absorber structure has a thickness of $0.0844\lambda_L$, where λ_L denotes the wavelength at the lowest frequency within the absorption bandwidth.

The parameters at the resonance points of the vanadium dioxide in the two states after optimization are shown in Table 1. There is one resonance peak in the dielectric state and two resonance peaks in the metallic state. The input impedance results of the absorber in the two vanadium dioxide states after optimization are presented in Fig. 3(a).

The curve of absorber absorptivity and reflection coefficient before and after the phase transition is shown in Fig. 3(b). The black curves represent the reflection coefficient and absorption rate prior to the phase transition, while the red curves correspond to the post-transition state. When the vanadium dioxide is in a high-resistance state, broadband with a reflection coefficient of less than -10 dB in the low-frequency range of 20.0–27.7 GHz is obtained. This is because vanadium dioxide acts as a special medium in its dielectric state, with its impedance real part approaching zero and hardly participating in absorption frequency selection. Thus, the patterned graphene acts as a frequency selector, stabilizing the real impedance of the graphene at 500 Ω between 20.0 GHz and 27.7 GHz. After the phase transition of the vanadium dioxide to a low-resistance state, a wide band with a reflection coefficient of less than 10 dB in the high-frequency range of 31.1–48.7 GHz is obtained. The vanadium dioxide is in a metallic state and participates in frequency selection with the graphene, generating double resonance. Therefore, when the vanadium dioxide is in a high-resistance state, it can be used as a low-frequency broadband absorber. When the vanadium dioxide undergoes a phase transition, it acts as a high-frequency broadband absorber.

TABLE 1. Equivalent capacitance and inductance at resonance of the two states of the vanadium.

	L (nH)	C (pF)	frequency
Dielectric state	0.511	82.17	24.8 GHz
Metal state 1	0.1287	165.6	34.48 GHz
Metal state 2	0.03254	449	41.64 GHz

2.3. The Regulation of Absorbers by Graphene

In addition to serving as a frequency-selective surface and absorption material, graphene also changes the carrier concentration, increases the Fermi level, and reduces its square resistance value by applying a bias voltage. This achieves the effect of managing the real part of the input impedance of the absorber, which consequently regulates the absorption frequency. By in-

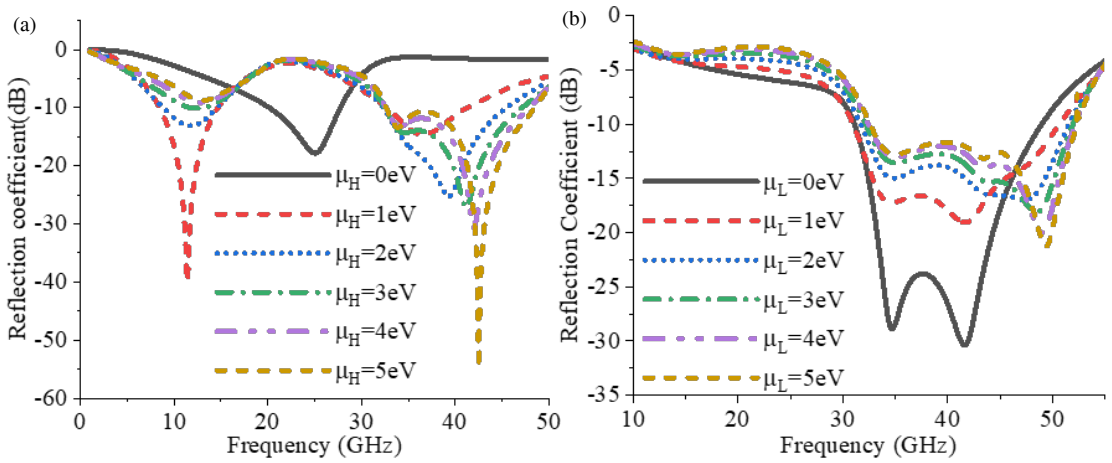

FIGURE 4. Reflection coefficient curves under different blocking states and different graphene Fermi levels. (a) High impedance state. (b) Low resistance state.

creasing its Fermi level, the square resistance of the graphene decreases, resulting only in a decrease in the real part resistance of the input impedance. As Fig. 3(a) reveals, the absorption frequency shifts toward a direction higher than the real part of the original impedance.

Figure 4 indicates the relationship between the Fermi level of the graphene (E_F) and the reflection coefficient of the absorber before and after phase transition. When $E_F = 0$ eV, the normal reflection coefficient result occurs. At $E_F = 1$ eV, before the phase transition of the vanadium dioxide, the reflection coefficient is the smallest at 11.4 GHz, while there is also a reflection coefficient below 10 dB at 41 GHz. After the phase transition of the vanadium dioxide, the overall reflection coefficient increases, and the absorption effect deteriorates. As the Fermi level continues to rise, before the phase transition of vanadium dioxide, the reflection coefficient at 11.4 GHz gradually increases. Moreover, above 41 GHz, the reflection coefficient steadily falls. More specifically, the reflection coefficient of $E_F = 5$ eV at 42.5 GHz is 54.67 dB. After the phase transition of the vanadium dioxide, the resonant frequency shifts blue, and the bandwidth below -10 dB increases by 4 GHz. However, due to the overall increase in the reflection coefficient, the absorption effect is slightly worse. Therefore, according to Fig. 3(a) and Fig. 4, before the phase transition of the vanadium dioxide, an increase in the Fermi level of the graphene reduces the square resistance. This causes the absorption frequency to shift toward the higher impedance real part on both sides, achieving a tunable absorption frequency for the absorber. After the phase transition of the vanadium dioxide, an increase in the Fermi level of the graphene amplifies the absorption bandwidth and blue shifts the resonant frequency. However, because of the increase in the reflection coefficient, the absorption rate falls.

In summary, the tunability of the graphene greatly increases the absorption capacity and application potential of absorbers.

2.4. Analysis of Angular Stability

To enhance the practicality of the absorber in this study, the absorber unit is designed with a symmetrical structure. Fig. 5 verifies that in both TE and TM polarization modes, the reflection coefficient of the absorber remains unchanged before and after the vanadium dioxide phase transition. Therefore, the absorber possesses excellent polarization insensitivity.

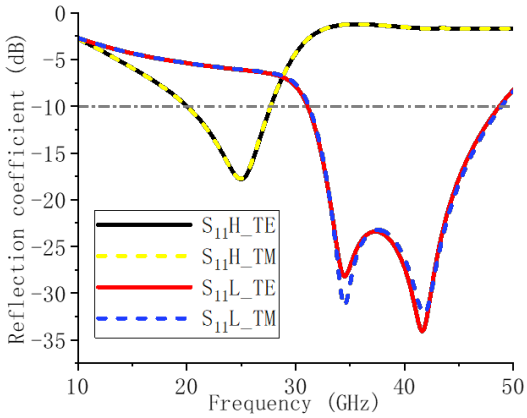

FIGURE 5. Reflection coefficient curves before and after phase transition under TE and TM.

The incident angle of the incident electromagnetic wave significantly impacts the reflection coefficient of the absorber, as Fig. 6 reveals. The reflection coefficient of the absorber is stable within 40° before the vanadium dioxide phase transition. After the phase transition of the vanadium dioxide, the incident angle is within the range of 0°–60°, and it has a stable reflection coefficient.

3. COMPARISON OF RESULTS

To further demonstrate the superiority of our dual-band switched tunable absorber, Table 2 presents a performance comparison of recently developed absorbers with similar adjustable functions. The proposed absorber in this study uses dual tunable materials of vanadium dioxide and graphene. Compared with most existing absorbers that realize broadband absorption in the metal state of vanadium dioxide and total reflection tunable function in the medium state, our design achieves broadband switchable absorption between the metal

TABLE 2. Performance comparison of recently developed absorbers with similar adjustable functions.

	Tunable material	Absorption band (relative bandwidth)		Graphene μ	thickness
1	VO_2	3.06–7.61 THz (84.55%)	Four frequency bands		$0.1415\lambda_L$
14	VO_2	3.1–7.45 THz (82.46%)	/		$0.0889\lambda_L$
16	VO_2	3.52–10.78 THz (101.54%)	/		$0.0945\lambda_L$
17	VO_2	0.66–1.84 THz (94.4%)	/		$0.0889\lambda_L$
18	VO_2 and Graphene	3.74–6.96 THz (60.19%)	/	0.8 eV	$0.1622\lambda_L$
28	VO_2	2.82–9.17 THz (105.92%)	/		$0.079\lambda_L$
29	VO_2 and Graphene	4.28–7.55 THz (55.28%)	5.5 THz and 7.5 THz	0.1/0.5 eV	$0.1297\lambda_L$
30	VO_2	1.27–2.64 THz (70.08%)	/		$0.0789\lambda_L$
This work	VO_2 and Graphene	31.1–52.27 GHz (50.79%)	20–27.7 (32.3%)/11.4 and 41 GHz	0–5 eV	$0.0844\lambda_L$

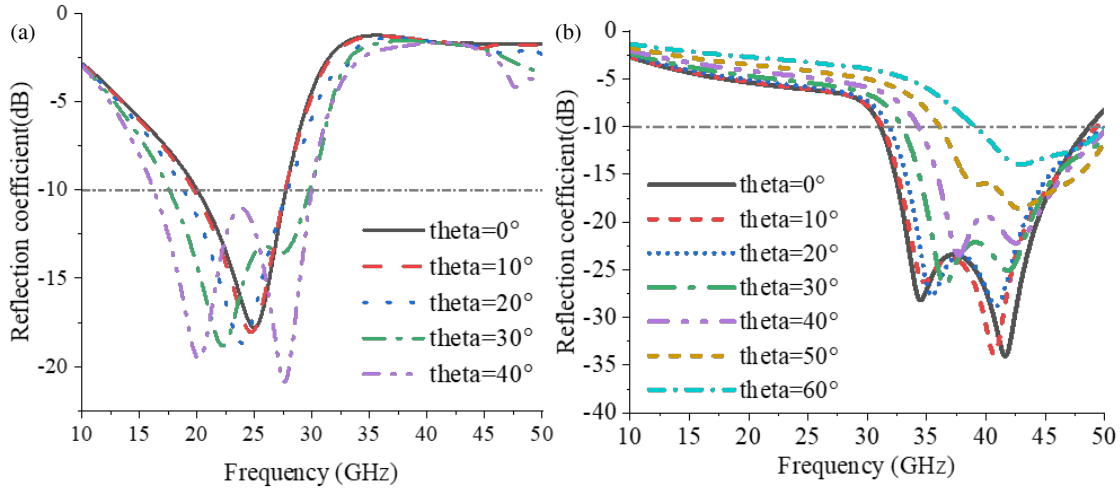

FIGURE 6. Relationship between the reflection coefficient and incident angle before and after the phase transition. (a) High impedance state. (b) Low resistance state.

state and medium state of vanadium dioxide. The advantage of our proposed absorber is that broadband absorption can also be achieved in the medium state, offering absorption ability at normal temperatures, rather than the total reflection surface function described in [10, 14], etc. The tunability of graphene enables absorbers to achieve tuning of the absorption frequency and bandwidth, thereby increasing the application capability of the absorber. Compared with the specific Fermi level in [13] and [16], the absorber designed in this paper regulates the Fermi level of the graphene over a wide range to achieve various absorption effects and enhance its application capabilities.

4. CONCLUSION

The dual-band switchable tunable absorber designed in this article is analyzed by constructing an equivalent circuit model and conducting a preliminary analysis of the unit structure. After simulation optimization, the specific parameters of the unit structure are determined. Based on the phase transition characteristics of the vanadium dioxide, with an absorption rate exceeding 90% at 20.0–27.7 GHz. After the high-temperature phase transition, the absorption rate exceeds 90% at 31.1–48.7 GHz. By increasing the Fermi level of the graphene, tuning the absorption frequency up to 11.4 GHz and 42.5 GHz can be achieved when the vanadium dioxide is in the dielectric state. Furthermore, tuning of the absorption bandwidth can be achieved when the vanadium dioxide is in the metallic state, with a maximum broadening of 4 GHz. The absorber designed in this study has an ultra-wide absorption frequency band, excellent tunability, and multifunctional absorption ability, which gives it broad application prospects.

ACKNOWLEDGEMENT

This work was supported in part by the Natural Science Project of Liaoning Education Department under Grant ID LJKZ0485.

REFERENCES

[1] Niu, J., Q. Yao, W. Mo, C. Li, and T. Chen, "Switchable terahertz absorber based on vanadium dioxide for bandwidth tunable broadband absorption and four-band absorption," *Journal of Physics D: Applied Physics*, Vol. 56, No. 39, 395101, 2023.

[2] Ma, Y. L., W. P. Wan, Z. B. Wang, Q. Chen, Y. J. Zheng, T. T. Guo, C. Y. Shuai, and Y. Q. Fu, "Broadband phase-modulated metasurface based on vanadium dioxide patches in microwave band," *AIP Advances*, Vol. 13, No. 4, 045214, Apr. 2023.

[3] Sheng, L. L., W. P. Cao, L. R. Mei, S. Zhang, Y. Lin, and L. Lu, "A low profile beam controling antenna based on digital metasurface," *Chinese Journal of Radio Science*, Vol. 36, No. 6, 938–946, 2021.

[4] Chen, H., W. Ma, Z. Huang, Y. Zhang, Y. Huang, and Y. Chen, "Graphene-based materials toward microwave and terahertz absorbing stealth technologies," *Advanced Optical Materials*, Vol. 7, No. 8, 1801318, 2019.

[5] Mapleback, B. J., K. J. Nicholson, M. Taha, T. C. Baum, and K. Ghorbani, "Complex permittivity and permeability of vanadium dioxide at microwave frequencies," *IEEE Transactions on Microwave Theory and Techniques*, Vol. 67, No. 7, 2805–2811, Jul. 2019.

[6] Hu, B. J., M. Huang, and H. W. Ding, "A three band dual tuned absorber based on Dirac semimetals and vanadium dioxide," *Journal of Infrared and Millimeter Waves*, Vol. 42, No. 02, 215–222, 2023.

[7] Huang, C. C., Y. G. Zhang, and L. J. Liang, "Narrow/broadband switchable graphene vanadium dioxide composite structure terahertz absorber," *Journal of Optics*, Vol. 42, No. 19, 7, 2022.

[8] Liu, C. B., J. Yin, and S. Zhang, "Temperature-tunable THz metamaterial absorber based on vanadium dioxide," *Infrared Physics & Technology*, Vol. 119, 103939, 2021.

[9] Xu, Z. and Y. Zhao, "A tunable dual broadband terahertz metamaterial absorber based on vanadium dioxide," *Journal of Beijing University of Chemical Technology*, Vol. 50, No. 4, 107–112, 2023.

[10] Xu, C., G. Duan, W. Xu, X. Wang, Y. Huang, X. Zhang, H. Zhu, and B.-X. Wang, "Thermally tunable vanadium-dioxide-based broadband metamaterial absorber with switchable functionality in the terahertz band," *Functional Composites and Structures*, Vol. 5, No. 2, 025004, 2023.

[11] Zhang, P., X.-H. Deng, L. Tao, P. Li, M. Lu, F. Guo, Y. Song, and J. Yuan, "Broadband actively tunable metamaterial absorber based on vanadium dioxide and Fabry-Perot cavity," *Optical Materials*, Vol. 138, 113716, 2023.

[12] Zou, Y., H. Lin, Y. Wu, H. Zhu, X. Zhang, and B.-X. Wang, "Theoretical investigation of an ultra-wideband tunable metamaterial absorber based on four identical vanadium dioxide resonators in the terahertz band," *Journal of Electronic Materials*, Vol. 52, No. 4, 2852–2864, 2023.

[13] Gevorgyan, L., H. Haroyan, H. Parsamyan, and K. Nerkararyan, "Tunable ultra-broadband terahertz metamaterial absorber based on vanadium dioxide strips," *RSC Advances*, Vol. 13, No. 18, 11 948–11 958, 2023.

[14] Nie, S., H. Feng, X. Li, P. Sun, Y. Zhou, L. Su, L. Ran, and Y. Gao, "A broadband absorber with multiple tunable functions for terahertz band based on graphene and vanadium dioxide," *Diamond and Related Materials*, Vol. 139, 110374, 2023.

[15] Lu, Z., Y. Zhang, H. Wang, C. Xia, Y. Liu, S. Dou, Y. Li, and J. Tan, "Transparent thermally tunable microwave absorber prototype based on patterned VO_2 film," *Engineering*, Vol. 29, 198–206, 2023.

[16] Wang, Z. B., Q. Chen, and Y. Q. Fu, "Design of broadband reconfigurable absorbing metasurfaces based on vanadium dioxide," in *Proceedings of the 2022 National Microwave and Millimeter Wave Conference of the Chinese Electronics Society*, Vol. 1, School of Electronic Science, National University of Defense Technology, 2022.

[17] Zhang, H., F. Liu, Y. Ma, A. Zhang, and K. Zhang, "Tunable and switchable terahertz absorber based on photoconductive silicon and vanadium dioxide," *Optics & Laser Technology*, Vol. 163, 109329, 2023.

[18] Yang, G., F. Yan, X. Du, T. Li, W. Wang, Y. Lv, H. Zhou, and Y. Hou, "Tunable broadband terahertz metamaterial absorber based on vanadium dioxide," *AIP Advances*, Vol. 12, No. 4, 045219, Apr. 2022.

[19] Wang, Q. Z., S. Y. Liu, G. J. Ren, H. W. Zhang, S. C. Liu, and J. Q. Yao, "Multi-parameter tunable terahertz absorber based on graphene and vanadium dioxide," *Optics Communications*, Vol. 494, 127050, 2021.

[20] Chen, W., C. Li, D. Wang, W. An, S. Gao, C. Zhang, and S. Guo, "Tunable wideband-narrowband switchable absorber based on vanadium dioxide and graphene," *Optics Express*, Vol. 30, No. 23, 41 328–41 339, 2022.

[21] Ri, C.-S., H.-J. Yun, S.-J. Im, and Y.-H. Han, "Bandwidth analysis of microwave metamaterial absorber with a resistive frequency selective surface by using an equivalent circuit model," *AEU — International Journal of Electronics and Communications*, Vol. 148, 154160, 2022.

[22] Garg, P. and P. Jain, "Analysis of a novel Metamaterial Absorber using equivalent circuit model operating at 3.5 GHz," in *2020 IEEE International Conference on Computational Electromagnetics (ICCEM)*, 246–247, Singapore, 2020.

[23] Li, Y.-H., L.-W. Deng, H. Luo, L.-H. He, J. He, Y.-C. Xu, and S.-X. Huang, "Equivalent circuit model and microwave reflection loss mechanism of double-layer spiral-ring metasurface embedded composite microwave absorber," *Acta Physica Sinica*, Vol. 68, No. 9, 095201, 2019.

[24] Wang, Y., Y. Chen, F. Liu, L. Chen, K. Ji, X. Wang, and X. Ji, "Vanadium dioxide enabled polarization insensitive tunable broadband terahertz metamaterial absorber," *Scientific Reports*, Vol. 15, No. 1, 10140, 2025.

[25] Shakiba, L. and M. R. Salehi, "Theoretical investigation of a multifunctional tunable terahertz metamaterial absorber based on vanadium dioxide and graphene," *Optical and Quantum Electronics*, Vol. 57, No. 3, 199, 2025.

[26] Afra, T., W. Fuscaldo, D. C. Zografopoulos, T. Natale, and F. Dell'Olio, "Tunable wide band near-perfect absorber for terahertz waves based on a vanadium dioxide metasurface," *Optical and Quantum Electronics*, Vol. 57, No. 5, 272, 2025.